Factory Radio Design of a 5G Network in Offline Mode

Citation for the original published paper (version of record):
Bärring, M., Iupikov, O., Glazunov, A. et al (2021). Factory Radio Design of a 5G Network in Offline Mode. IEEE Access, 9: 23095-23109. http://dx.doi.org/10.1109/ACCESS.2021.3055941

(article starts on next page)

IEEE Access
Multidisciplinary | Rapid Review | Open Access Journal

Received January 13, 2021, accepted January 24, 2021, date of publication February 1, 2021, date of current version February 9, 2021.

Digital Object Identifier 10.1109/ACCESS.2021.3055941

Factory Radio Design of a 5G Network in Offline Mode

MAJA BÄRRING[1], OLEG IUPIKOV[2], (Member, IEEE), ANDRÉS ALAYÓN GLAZUNOV[2,3], (Senior Member, IEEE), MARIANNA IVASHINA[2], (Senior Member, IEEE), JONATAN BERGLUND[1], BJÖRN JOHANSSON[1], JOHAN STAHRE[1], FREDRIK HARRYSSON[4], (Senior Member, IEEE), ULRIKA ENGSTRÖM[4], AND MARTIN FRIIS[5]

[1]Department of Industrial and Materials Science, Chalmers University of Technology, 41296 Gothenburg, Sweden
[2]Department of Electrical Engineering, Chalmers University of Technology, 412 96 Gothenburg, Sweden
[3]Department of Electrical Engineering, University of Twente, 7500 AE Enschede, The Netherlands
[4]Ericsson Research, Ericsson, 417 56 Gothenburg, Sweden
[5]Manufacturing Development Centre, SKF, 415 50 Gothenburg, Sweden

Corresponding author: Maja Bärring (maja.barring@chalmers.se)

This work was supported by the National, Digital Industrial Pilot Program operated by the Swedish Agency for Innovation Systems (VINNOVA) through the 5G Enabled Manufacturing (5GEM) Project, under Grant 2015-06755.

ABSTRACT The manufacturing industry is connecting people and equipment with new digital technologies, enabling a more continuous stream of data to represent processes. With more things connected, the interest in a connectivity solution that can support communication with high reliability and availability will increase. The fifth generation of telecommunication, i.e., 5G has promising features to deliver this, but the factory environment introduces new challenges to ensure reliable radio coverage. This will require efficient ways to plan the Factory Radio Design prior to installation. 3D laser scanning is used at an ever-increasing rate for capturing the spatial geometry in a virtual representation to perform layout planning of factories. This paper presents how to combine 3D laser scanning and physical optics (PO) for planning the Factory Radio Design of a cellular Long-Term Evolution (LTE) network (5G) in a virtual environment. 3D laser scanning is applied to obtain the spatial data of the factory and the virtual representation serves as the environment where PO computation techniques can be performed. The simulation result is validated in this paper by comparison to measurements of the installed network and empirical propagation models. The results of the study show promising opportunities to simulate the radio coverage in a virtual representation of a factory environment.

INDEX TERMS 3D laser scanning, 5G, factory radio design, Industry 4.0, long-term evolution (LTE), physical optics (PO), smart manufacturing (SM).

I. INTRODUCTION

Anything that can benefit from having a connection is expected to have one in the future [1] and with an increasing amount of things being connected, they will also have a greater impact on how mobile and wireless communication systems are used [2]. Machine-to-machine (M2M) and machine-to-person communication will be delivered by the Internet of Things (IoT) technologies offering values in terms of improved efficiency, sustainability, and safety for both the industry and for the society at large [3]. IoT provides the possibility of connecting devices directly to the Internet and the trend is also seen in the industry. In the industrial domain are the components hardened compared to other areas using IoT to serve the industrial environment and it is referred to as Industrial Internet of Things or Industrial IoT (IIoT). The components involve sensors or actuators and mobile equipment such as smartphones, tablets, and smart glasses [4]. Besides the increased capabilities, the connectivity-based services are simultaneously also becoming affordable with an annual decreasing cost for M2M modules. With more devices and people connected, the mobile system will have to deal with demands for constant availability, high resilience, wide-coverage, low latency, and large bandwidth [1]. Great challenges of the future network will be to meet higher traffic volume for indoor and outdoor environments, traffic

The associate editor coordinating the review of this manuscript and approving it for publication was Santi C. Pavone.

asymmetry, and efficiency in the spectrum, energy, and cost [5]. A network that will provide a 1000 times capacity increase, support 10-100 times more connected devices, and reduce the end-to-end latency by five times, is 5G and this promising development will support IoT and the communication between devices [6].

The procedure of planning a network for the indoor environment has often been governed by the rule of thumb based on the intuition to fulfill the basic services [2], [7]. The promising features of 5G will, however, only be realized if the value that can be gained exceeds the deployment costs of the network while meeting the Quality of Service (QoS) requirements to the end-users [6]. A factory setting introduces new aspects affecting the network performance that should be considered in the network planning processes. For example, machines and equipment are influencing the propagation of radio waves, due to the scattering of the electromagnetic signals. In addition, when new equipment is installed or changes are made in the production system, this interrupts production and impacts on productivity and ability to deliver in time [8].

In order to deliver the desired network performance in a factory environment, it is therefore essential to perform cost-efficient network planning based on accurate electromagnetic (EM) wave propagation models and algorithms [9]. Geometrical models of the indoor environment can be extracted from point clouds and then be used in EM field simulation tools to predict the propagation of radio waves [10]. The EM simulations can include multiple reflections, diffraction, and scattering effects in the given environment as well as actual permittivity and conductivity at different points, thereby providing much higher accuracy and generality than conventional data-based estimation techniques [11].

This paper introduces a planning approach in an offline mode. The developed methodology is evaluated in the presented study. The approach is focused on the radio design planning of a 5G network (a mobile LTE network with 5G characteristics) for a factory environment in an offline mode. It is a combination of two main components: 1) 3D laser scanning to capture the spatial data of a factory environment, i.e., position and shapes of walls, ceiling, floor, and other objects, and 2) prediction of EM radio wave propagation by means of PO computations. The research question posed here is ''Can a planning approach in an offline mode provide the simulation results required for ensuring a reliable and available network in the physical environment?'' The simulated results are compared to measurements of the network performance in the physical setting and the comparison shows promising results of the approach developed.

The contribution of the paper is to identify a new network planning procedure of indoor factory environments while maintaining high accuracy and keeping disturbances of the production system to a minimum. The motivation for this is two-fold: (i) to support both Information and Communication Technology (ICT) providers in finding more efficient working procedures for planning a reliable and available network in a factory environment offline, and (ii) to limit the interruptions of a production system under deployment, which is of great importance for manufacturers. There are few prior studies investigating this opportunity to plan a mobile network for a factory setting offline, but it will be a growing area of interest for manufacturers and ICT providers as the need for connected factories increases.

The remainder of the paper is divided into five sections. In Section 2, related work is presented on connectivity, network requirements and planning, and capturing spatial data with 3D laser scanning. Section 3 introduces the testbed project that the study has been part of and the technical characteristics of the 5G network used, to continue to present the planning approach in an offline mode in section 4. Here, the four steps that constitute the approach are thoroughly explained of how they were performed and the results received. Section 5 evaluates the results in order to understand the applicability of the approach; capture of spatial data, the measurements collected from the 5G network in the actual environment, and comparison to evaluate the accuracy of the simulation. The last section, 6, presents the concluding remark for this paper.

II. THEORETICAL BACKGROUND

A. CONNECTIVITY

The 3rd Generation Partnership Project (3GPP) is the active standardization body in defining the next generation of telecommunication, 5G, in the same way as they were active in standardizing the LTE network [12]. Based on the definition proposed by 3GPP, LTE is a highly flexible radio interface and was an integral part of the advancement of what became 4G [13], [14]. With the introduction of mobile services based on 4G LTE, users of the mobile network could experience the same type of responsive Internet browsing that previously only was possible on wired broadband connections. This is a reason for the steady expansion of 4G LTE across global markets [15] and is a motivator for the urge in technologies that will define 5G [16]. Attention is now turning towards future 5G mobile broadband technologies and standards.

The main driver for guiding the commercial rollout of the 5G wireless system is the introduction of a wide variety of new emerging applications and is expected to provide network solutions in both public and private sectors. These sectors include energy, agriculture, city management, health care, manufacturing, and transport [17]. The new network challenges that 5G will need to encounter involve not only the increased number of devices to be served but also the diverse nature of devices and the service requirements each of them pose [18]. Another development that is expected with 5G is the transition to evaluate the network performance on not solely hard metrics, meaning peak data rates, coverage, and spectral efficiency, but expand towards including user's Quality of Experience (QoE). This will for instance involve the ease of connectivity with nearby devices and higher energy efficiency [15].

The current transformation taking place in manufacturing is dependent on a connectivity solution that can provide an end-to-end networking infrastructure to support smart manufacturing operations [19]. 5G is expected to be an integral part of this networking infrastructure, serving the needs of both within and outside of the factory requirements [20]. The in-factory setting includes scenarios of automation production and industrial control, and more specific applications are for instance communication and control of automated guide vehicles (AGVs), edge-computing systems to serve time-critical operations at the machine level, as well as maintenance operations of production systems to ensure availability of equipment [21]–[24].

To address the demands and requirements that have been identified for mobile communication in 2020 and beyond, 5G will rely on a portfolio of access and connectivity solutions [25]. Existing technologies will be the foundation for 5G complemented by new radio concepts such as Massive Multiple-Input and Multiple-Output (MIMO), Ultra-Dense Networks, Moving Networks, Device-to-Device, Ultra-Reliable, and Massive Machine Communications [2]. Mobile and wireless communication need to fulfill requirements posed by both the human and machine-type communication that involves cost, high complexity, energy consumption, and services. For the machine area, the requirements mainly involve supporting a density increase of devices connected in the same area generating in the context low volumes of data with a sporadic time interval [26]. The new application areas will imply much higher demands on the reliability of the connectivity compared to what communication does today [27].

B. PLANNING OF THE NETWORK FOR AN INDOOR ENVIRONMENT

Network planning is an iterative process that aims to ensure a network that can meet the needs of subscribers and operators of the network and solve a multi-objective optimization problem that considers parameters such as technological, economical, and demographical. The state-of-the-art in this research area shows that planning and performing maintenance of telecommunication networks are in constant demand for better solutions, where costs should be reduced at the same time as the level of service should be guaranteed [28].

Most network planning methods used today are designed to ensure the coverage for an outdoor environment, but as the demand for networks in indoor environments increases, methods are needed that can handle the complexity posed in these environments to ensure expected network performance [29]. Measurements of the radio channel and propagation channel modeling derived from measurements represent the reality and provide the best indications of the actual radio coverage [30]. Since this is a complicated endeavor, dependent on quality equipment and other resources, site-specific simulations of the radio wave propagation that requires a limited amount of measurements for the analysis will be a key enabler [31]. To accurately model the radio channels for an indoor environment requires consideration of the multipath propagation that appears due to the physical objects with different electrical properties, sizes, and shapes that exist in the environment [32]. There are various approaches to predict or simulate the propagation of EM waves for wireless communications applications [9] and an effective approach to characterize the propagation of millimeters waves (mmWave) for the indoor environment is deterministic ray tracing [33]. To apply ray tracing requires an accurate 3D representation of the environment, with information on materials and object properties [29]. Virk *et al.* [31] have approached this key research area of performing site-specific radio propagation simulations for coverage analysis with the use of ray tracing and point cloud. The challenges of achieving an appropriate radio propagation simulation heavily rely on having an accurate representation of the environment and the electrical properties of the material present. They present a method for on-site permittivity estimation in built environments, which involves ray tracing in an accurate 3D description of the environment in a point cloud. This will identify scatterer in the environment and estimate the permittivity of the network.

1) RAY-BASED AND PHYSICAL OPTICS METHODS

There are two basic ray-based approaches to searching propagation paths in an arbitrary model of an environment with objects that are much larger than the wavelength of the carrier frequency. The so-called ray tracing and ray launching are techniques commonly used to simulate wave propagation in a deterministic manner for a given geometry of the environment. The ray tracing is more a point-to-point computation since it finds valid propagation paths between the receiver and the transmitter. On the other hand, ray launching is an area-oriented algorithm where rays are launched from a fixed transmitter position in all relevant directions and discretized into small angular increments. There are many different ways to implement such an approach with different advantages and disadvantages, but in general, it means finding each possible propagation path or ray (to some predetermined accuracy) between a transmitter point and a receiver point via interactions such as transmission, shadowing, reflections, diffractions, and scattering of intermediate and surrounding objects in the environment. Once the ray paths are determined, the EM properties are calculated by theory for intermediate interactions with objects, e.g., image theory, Fresnel reflection theory, and diffraction theory [34]. The accuracy of such a model is directly related to the amount of detail in the geometrical description or the environment, material description, and on the accuracy of the models for object interaction. With an environment, such as an industrial environment, the geometrical representation of obstacles in the environment may become very large, which means that the calculation effort increases tremendously. In practice, this problem is often treated by methods to reduce geometry complexity or sort rays in respect of [35].

A possibly more tractable and direct method is based on physical optics [34]. Instead of calculating bounces and

interactions of rays and using specific models for interactions, in physical optics objects that are visible from the transmitter are "painted" with an equivalent current found from the impinging EM field in the first interaction that re-radiates the field. In a number of subsequent steps, this procedure is repeated with a discretization of each obstacle becoming a new radiator. This method requires less "ray tracing" but instead the calculation effort increases rapidly in each interaction depending on the necessary discretization of obstacles. There are also various hybrid methods that also may utilize statistical methods or fast optimization algorithms and iterative techniques [36], [37] to reduce computational effort and increase prediction efficiency. A common issue is, however, the accuracy of a geometric model of the environment and to what extent this can be reduced to increase efficiency for tractable calculation effort, and, at the same time, reach the required accuracy for a good prediction of radio network coverage and performance. This is a topic for study, especially in a very complex environment that is expected in an industrial context. A challenge for a good radio propagation study is also the consideration of the material in an environment that will have an impact on the scattering effects as well as the spatial data.

C. CAPTURING SPATIAL DATA WITH 3D LASER SCANNING

Numerous technologies for capturing spatial data are available and they can be categorized into tactile and non-contact methods. The tactile method interacts with the surface of interest by, e.g., a mechanical probe and the non-contact methods are using light, sound, or magnetic fields to collect data about the surface [38]. Within the non-contact methods, there are active and passive sensors. Active sensors emit a media that interacts with the object of interest to obtain the spatial data. Passive sensors instead rely on existing media, such as the ambient light as the signal. Examples of active non-contact sensors are structured light scanners and 3D laser scanners; an example of a passive sensor is a digital camera [38], [39]. 3D laser scanning, also called Light Detection and Ranging (LiDAR), is a technology that can serve the purpose of capturing spatial data in three dimensions and it has become a key technology in several areas for this purpose [39], [40]. 3D laser scanning is an active technology that uses laser light to calculate the distance to an object by capturing the reflection of the emitted laser as it hits the surface of the object. To capture 3D spatial data of the surrounding area, the laser beam is systematically directed across the surrounding environment using a rotating mirror. Distance measurements are captured at a rate of up to hundreds of thousands of points per second as the laser beam traverses the surroundings. For each measurement, its direction and distance are stored in the form of a 3D point [39], [41]. The 3D laser scanning technology is capable of collecting 3D coordinates automatically and systematically in the range of one up to hundreds of meters in distance. The principles applied are either time-of-flight or phase comparison measurements [38].

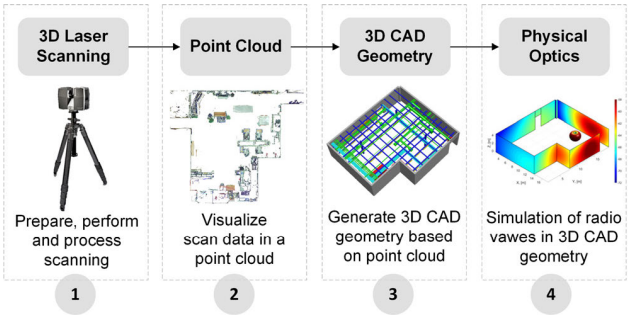

FIGURE 1. The individual steps, step 1 to 4, of the offline planning approach.

III. 5G ENABLED MANUFACTURING – A TESTBED PROJECT

This study has been performed within the testbed project 5G Enabled Manufacturing (5GEM), where Chalmers University of Technology (hereafter referred to as Chalmers), as an academic partner, has collaborated with SKF, a bearing manufacturer, and Ericsson, a telecommunication company and ICT provider. The question raised in this project has been "What if we had unlimited free connectivity on the shop floor, what could we then do?" The unlimited free connectivity, in this case, has been modeled by Ericsson's state-of-the-art LTE end-to-end network with 5G characteristics and components, including both central and distributed core and cloud. The main objective has been to investigate how 4G/5G cellular technologies can support to increase efficiency, flexibility, traceability, and sustainability in the manufacturing context. This has been performed by the identification and development of four demonstrators that can exemplify how the connectivity can improve the performance measures mentioned. The demonstrators are (A) Factory Radio Design, (B) Network and Cloud, (C) Stationary Equipment Connectivity, and (D) Mobile Connectivity. Besides affecting the performance measures, the different demonstrators also influence the different phases (operation, maintenance, and design phase) of a production system.

This study has only involved demonstrator (A) Factory Radio Design, which is relevant in the design phase of the production system, either in the Greenfield phase for a new production system or in the Brownfield phase where the existing system is redesigned. It is believed that if the ray-tracing simulation could be performed in a virtual representation of a factory, this could provide a procedure that can be both more accurate and more efficient in terms of time and resources compared to how the planning and installation of the network are done today. The goal of this demonstrator is to develop an offline approach to design the radio installation and the steps of the approach are visualized in Fig.1. An LTE network with Ericsson equipment was installed at the Chalmers Smart Industry laboratory (CSI-lab). Two LTE Radio Dots comprising antenna functionality and providing indoor radio coverage were connected to the radio, baseband, and network core units. Connection to the Ericsson network in a nearby building was done over the air via MINI LINK.

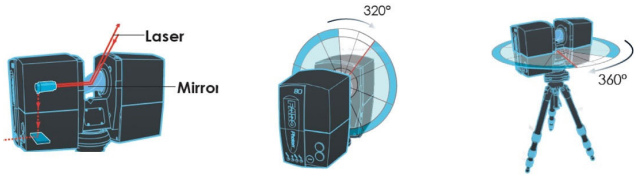

FIGURE 2. FARO 3D Laser Scanner [42].

The indoor radio spectrum used was 20 MHz at LTE TDD B40 (2355-2375 MHz).

IV. OFFLINE PLANNING APPROACH FOR FACTORY RADIO SPACE DESIGN

The four steps of the approach are visualized in Fig. 1. This approach is developed to support both the case when a 5G network should be planned for an existing production system (with machines and equipment in place) and in the case of designing a new production system (with a planned layout including machine and equipment). The procedure of the approach is the same for both cases (existing and new production system) following steps 1-4. Spatial data covers the three first steps of the method where a virtual representation of the environment is developed. The fourth step is when the physical optics simulation is performed. The remaining part of this chapter will explain the steps in more detail how they were performed, what assumptions were made, and the results gained.

A. STEP 1-3: SPATIAL DATA COLLECTION AND VISUALIZATION

The 3D imaging data collection was conducted using a FARO Focus 3D laser scanner. It is a type of Terrestrial Laser Scanner (TLS) that uses an articulated 2D laser to gauge and record distance measurements. The device can capture surface samples systematically over a 360 by 320 degrees' field of view, see Fig. 2. A capture cycle typically involves 30-40 million data points with a positional accuracy of +-2 mm (as stated by the manufacturer FARO). The spatial data measurements are complemented by an RGB sensor that captures color information over the same field of view.

CSI-lab was used as the setting in this study and the laboratory environment contains equipment for teaching and a CNC machine. The laboratory measures 14.5 m by 18 m ($\sim$261 m^2) and the height of the ceiling varies between 3 m and 4.6 m. The building material in the laboratory contains to a large degree steel (pillars, ventilation system, whiteboards for teaching, beams that goes 0.4 m down from the ceiling, and a CNC machine) and sheet metal (cable ladders, fire extinguisher, gates, and interior). The ceiling contains sheet metal under a sound-absorbing material that covers 75% of the ceiling, the walls have a first layer in plaster and studs in steel that can be found behind the plaster with a 0.6 m spacing and the floor is in concrete with a plastic layer over it. Two Radio Dots were installed in the laboratory on a height of 2.9 m from the floor, on cable ladders. Table 1 provides an overview of the data collection metrics. The data collection

TABLE 1. 3D imaging capture and processing data.

Number of scans		10
Million data points	**Per scan**	10*10^6
	In total	100*10^6
Data size	**Raw files**	650 MB
	Processed	1.1 GB
Time duration for	**Capture**	3 h
	Processing	3 h

FIGURE 3. Step 1-3 From Scanning to CAD representation of the laboratory that serves as a test facility. The red circle marks the LTE Radio Dot installation position.

of the spatial data for the laboratory was conducted during a three-hour session with a total number of ten scans and there was no other activity in the area during the duration of the scanning.

The scan data was processed at Chalmers using the Autodesk ReCap software. An overview of the production area as visualized in the software can be seen in Fig. 3. The processed data set was used to generate a combined point cloud file covering the entire production area. The combined point cloud was further exported to a neutral data format e57 (ASTM) and sub-sequentially imported into Autodesk ReCap for visualization and saved as .rcp data files to be used in Autodesk CAD as blueprints for creating simple CAD representations of the area. It should be noted that several comparable software alternatives can visualize point clouds and create CAD representations available off-the-shelf. The choice of Autodesk software was based on the following main criteria: 1) the ability to handle large amounts of point cloud data and 2) its compatibility with CAD software.

The option of automated meshing of the scan data was ruled out due to the level of complexity in the machine geometries and because the level of spatial detail was met by generating geometry sketches of the environment by manual efforts. For future solutions and implementations, it is desirable to develop automated processes to generate CAD geometry from the measurement data or perform analysis directly in the measurement data. The final CAD representation of CIS-lab with details about media infrastructure and other equipment can be seen in Fig. 3. The red circle marks in each step the location of Radio Dot no. 1, see Fig. 4 for the position of Radio Dots.

B. STEP 4: PHYSICAL OPTICS SIMULATION

In this study, we have used a hybrid Physical Optics (PO) method as initially developed for multi-scale reflector

TABLE 2. Simulation parameters for PO.

Simulation parameter	Setting
Frequency setting of interest	2.365 GHz
Size of the EM-problem	~332,000 mesh cells with a size of ~42 mm×42 mm (~0.33×0.33 wavelength)
No. of radio sources (Radio Dots)	Two Radio Dots at different positions on the ceiling, operating either one by one or simultaneously.
EM model	The environment consists of 10 walls.
E-field power distribution	Calculated on the measurement path data to enable comparison.

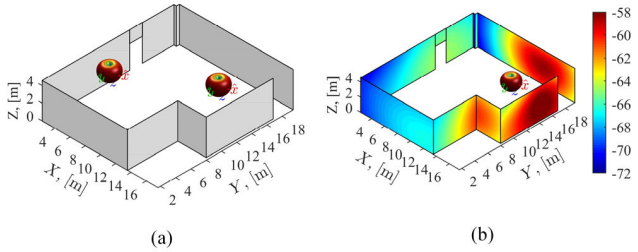

FIGURE 4. EM model of the lab: (a) PEC walls and radiation patterns of two Radio Dots; (b) Magnitude of the PO current induced by the upper Radio Dot in [dB].

antenna systems [36], where we have made the following simplifications to enable a time-efficient analysis of the considered in-door environment:

- Only flat and slowly curved surfaces of the scatterers are supported (e.g., walls, floor, and ceiling of the room). This can be easily extended by using other methods (MoM, CBFM, MLFMM, etc.) to compute current on electrically small or highly curved objects [36].
- The materials of the walls, floor, and ceiling of the rooms are assumed to be perfect electric conductors.
- Mutual coupling effects due to the scattering of radio waves in between the walls are negligible.
- The radiation pattern of the source is assumed to be a Gaussian pattern (linear-polarized) with the taper -1 dB at $\theta = 90°$.

This PO method has been implemented in MATLAB® and validated for several benchmarking examples in previous projects. For more details on the accuracy and simulation efficiency of this simulation method, the reader is referred to [36] and [43]. Furthermore, the simulation settings that were used to analyze the above-described environment are documented in Table 2.

Fig. 4 (a) shows the described geometrical model of the environment, as well as the position of two Radio Dots, represented as their radiation patterns. The magnitude of the PO current induced by the Radio Dot 1 on the walls is depicted in Fig. 4 (b).

Since we assumed no mutual coupling between walls in this simplified model, the field at any point inside the room can be calculated as a superposition of the field directly coming from the Radio Dot and the field scattered from the walls (radiated by the PO current). The magnitude distribution of

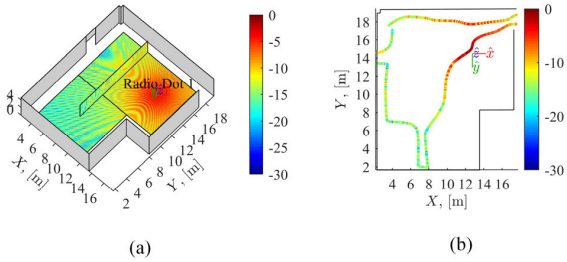

FIGURE 5. The magnitude of the E-field: (a) on a plane elevated 1 m over the floor, and on a vertical YZ-plane; and (b) along the measurement path in [dB].

the resulting E-field on a plane elevated 1 m over the floor and on a vertical YZ-plane is shown in Fig. 5.

V. EVALUATION OF RESULTS FROM THE OFFLINE PLANNING APPROACH

A. MEASUREMENTS OF THE INSTALLED NETWORK IN TEST ENVIRONMENT

Measurements of radio propagation from installed access points (Radio Dots) have been performed in CSI-lab by using a TEMS pocket LTE mobile phone User Equipment (UE) system for network testing, operating in the B40 band. The measurements were done by Ericsson with the TEMS pocket system. Network parameters such as Reference Signal Received Power (RSRP) can be measured (3GPP TS 36.214). RSRP is the received power averaged in linear scale (W) over reference symbol resource elements (RE) within the measurement bandwidth and given in dBm. As the name suggests, a reference signal exists as a single symbol at a time, the measurement is made only on the resource elements that contain the cell-specific reference signals. As such, the RSRP measurement bandwidth is the equivalent of only a single subcarrier of the OFDM transmission. The RSRP provides information about signal strength solely, i.e., no interference or noise information is taken into account. The reference point for the RSRP shall be the antenna connector of the UE. The RSRP can be logged while walking around in the environment, thus giving a map of how the received signal varies. The reporting range for RSRP is defined from -140 dBm to -44 dBm in 1 dB steps (i.e., resolution). RSRP measurements are used for cell selection, cell reselection, handover, mobility measurements and to obtain an estimate of the path loss for power control computations. Hence, modeling the RSRP level properly is essential for the design and optimization of LTE networks.

Since the measurements were performed indoors, using a GPS system for logging the actual position is not possible to exploit. Therefore, in these measurements, the position of the user holding the phone is repeatedly pinpointing positions on a map on the mobile phone screen by hand. The logged data could in a post-processing stage be aligned with interpolated positions to give a detailed description of signal strength at a specific position with fairly high accuracy. The LTE frequency band was B40, 2355-2375 MHz, i.e., 20 MHz

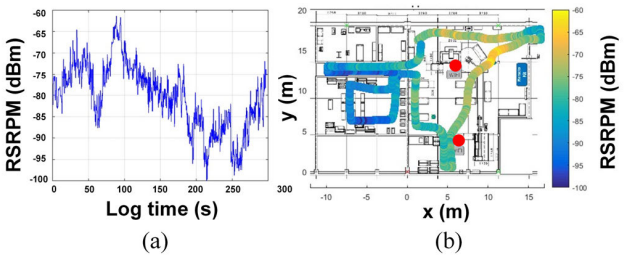

FIGURE 6. (a) Measurement path (RSVP vs time) and (b) averaged measurements results. Red points mark the LTE Radio Dot installation position.

transmission channel bandwidth (BW), and the output power was 20 dBm over 20 MHz. The RSRP measurements were performed both with single Radio Dots active and both active.

A Resource Element (RE) is one 15 kHz subcarrier times one symbol. REs aggregate into Resource Blocks (RBs). An RB has dimensions of subcarriers times symbols. Twelve consecutive subcarriers in the frequency domain and six or seven symbols in the time domain form each RB. Hence, there are $12 \times 7 = 84$ RE in a single RB in LTE. At the maximum channel BW of 20 MHz, the maximum number of RB is 100. Using these definitions and the RSRP definition above, the RSRP can be computed in dBm as the power received over the whole BW minus 10log (84×100), where RE $= 8400$ is the total number of RE at the 20 MHz bandwidth.

A snapshot of a measurement path (RSRP vs time) is shown in Fig. 6a. Averaged measurement results (as heat maps) with one Radio Dot active are shown in Fig. 6b. It should be noted that the measurement results correspond to measurement positions in the same room as the Radio Dot and the adjacent room. However, our analysis is concerned with data collected in the same room where the Radio Dots are deployed.

The measurement results show that the LTE coverage at CSI-lab is good, the best signal level is observed in the open hall where the Radio Dots are deployed. In addition, the measured receive power fluctuates along the measurement path, which is due to the perceived change in the radio environment when walking around due to, e.g., reflections in various metal structures.

B. COMPARISON OF SIMULATION RESULTS AND MEASUREMENTS OF NETWORK

In this section, the accuracy of the computational predictions of receive power levels by means of the PO simulations is evaluated and compared against measurements obtained in the live network deployed in the CSI-lab. In comparison, the log-distance path loss model - an empirical propagation model vastly used in the design and optimization of wireless networks, as well as the free-space propagation model are included [9]. The latter model has been taken into account since the considered propagation environment in this paper is a multipath Line-of-Sight (LoS) propagation channel. This means that there is a direct LoS path between the transmit (Tx) and the receive (Rx) antennas in addition to other multipath components.

TABLE 3. Empirical model parameters (1) and comparison to free-space model (2) at the frequency of interest f = 2.365 GHz.

Parameters	Lower Radio Dot	Upper Radio Dot	Free-Space
α, [dB]	39.8	42.6	40.8
γ	1.9	1.7	2
σS, [dB]	3.3	3.3	0

The empirical path loss model plus shadowing is a linear model in [dB]

$$L = \alpha + 10\gamma \log d_{\text{Tx - Rx}} + S \tag{1}$$

where the first two terms model the distance-dependent average path loss (average trend) and the third term models the path loss shadowing effects (fluctuations). The constant α depends on the environment, the antennas used, and the carrier frequency; it models the average path loss at a unit distance, e.g., at 1 m. The constant γ is the path loss exponent modeling the rate of decay of the average receive power with the separation distance between the receiver and the transmitter $d_{\text{Tx}-\text{Rx}}$. S is a Gaussian (also called normal) random variable with zero mean and standard deviation σS. The variable S emulates the fluctuations at a fixed distance $d_{\text{Tx}-\text{Rx}}$, usually due to large-scale fading, but can also be used to model the overall signal fluctuations including the small-scale fading [30]. The function log(.) is the logarithmic function with base 10. The values of α, γ, and σS are obtained by fitting (1) to the measurement data.

If there are no multipath components, i.e., then there is only a single LoS direct path between the transmitter and the receive antennas contributing to the received power. The free-space path loss model for isotropic antennas can be used, which expressed in [dB] is given by

$$L_0 = 32.4 + 20 \log f + 20 \log d_{\text{Tx-Rx}} \tag{2}$$

where f is the carrier frequency in [GHz] and the distance $d_{\text{Tx}-\text{Rx}}$ between the receiver and the transmitter is measured in [m].

Table 3 shows the obtained model parameters according to (1) estimated from measurement data. The polynomial curve fitting (polyfit) MATLAB®-function was used to obtain α and γ. The standard deviation σS was computed from the fitting residuals. By comparing (1) and (2) we readily obtain $\alpha = 40.82$ dB at the frequency of interest $f = 2.365$ GHz and $\gamma = 2$ for the free-space path loss model.

Fig. 7 shows the path loss as a function of the logarithm in base 10 of the separation distance between the receiver and the transmitter, when (a) the lower Radio Dot is active and (b) when the upper Radio Dot is active. Both the measurement data, the average fitting functions, and the free-space path loss are shown. As can be seen from both Table 3 and Fig. 7, results for the empirical path loss (i.e., the average trend)

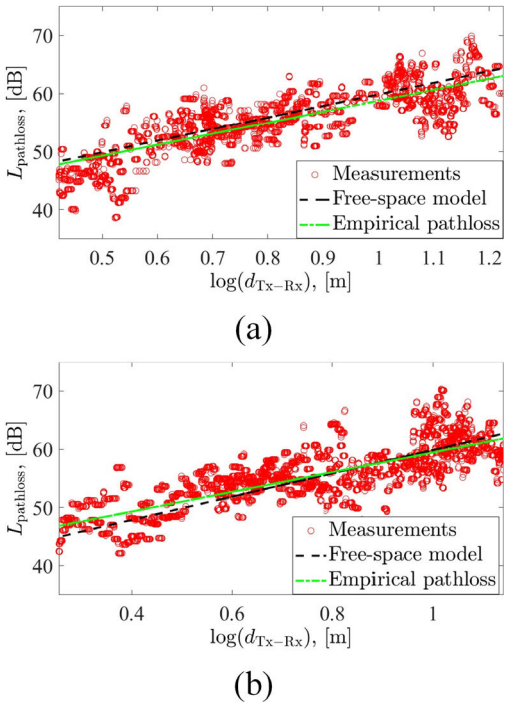

FIGURE 7. Path loss as a function of the logarithm of the separation distance between the receiver (R_X) and the transmitter (T_X), (a) when the lower Radio Dot is active, and (b) when the upper Radio Dot is active. See Fig. 4 for the Radio Dot positions.

and the free-space path loss are rather similar. This is to be expected since we are in the presence of a LoS propagation channel and the antennas installed in the Radio Dot systems ought to be rather uniform over a hemisphere covering the floor of the CSI-lab. The shadowing or fluctuations around the average log-distance trend is of the same magnitude in both cases since both Radio Dots are deployed in the same environment.

The path loss model plus shadowing is used to determine the receive power according to the well-known relationship

$$P_{\text{Rx}} = EIRP_{\text{Tx}} + G_{\text{Rx}} - L \tag{3}$$

where L is the propagation path loss, G_{Rx} is the gain of the receive antenna which in our case is the antenna of the TEMS pocket LTE mobile phone used with $G_{\text{Rx}} \approx 0$ dBi. The $EIRP_{\text{Tx}} = 20$ dBm is the equivalent isotropic radiated power over the channel bandwidth of 20 MHz. In free-space (3) is just the Friis equation.

In order to be able to fully compare the simulated data we need to evaluate the network-related parameter RSRP

$$P_{\text{rec}} = P_{\text{Rx}} - 10\log RE \tag{4}$$

where $RE = 8400$ is the total number of radio elements over the 20 MHz BW. Expressions (1)-(4) model the receive signal for a single active Radio Dot. If both Radio Dots are active, the total receive power is the sum in [W] from both transmitters. It can be shown [35] that the total receive power

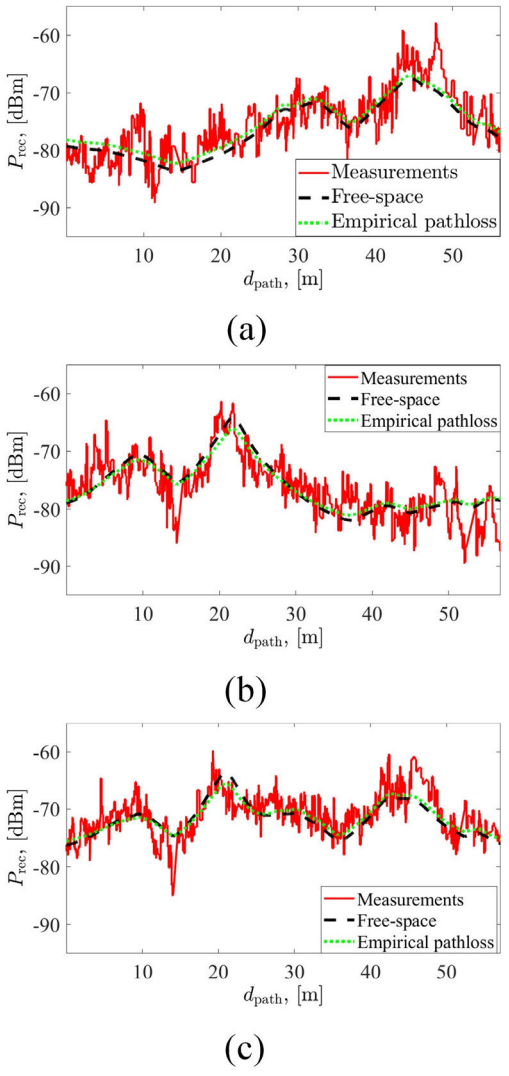

FIGURE 8. The received power (RSRP) as a function of the displacement along the measurement path, (a) when only the lower Radio Dot is active, (b) when only the upper Radio Dot is active, and (c) when both Radio Dots are active. See Fig. 4 for the Radio Dot positions.

expressed in [dBm] is then given by

$$P_{\text{rec}} = EIRP_{\text{Tx}} + G_{\text{Rx}} - 10\log RE - 10\log\frac{L_{\text{l}}L_{\text{u}}}{L_{\text{l}} + L_{\text{u}}} \tag{5}$$

where we have used that the transmit power from both Radio Dots is the same, L_{l} and L_{u} are the path loss corresponding to the lower and the upper Radio Dot, respectively. Expression (5) can be applied to both measurement and simulated data provided that the assumptions above hold for each specific case.

Fig. 8 shows the receive power (in our case the RSRP obtained from equations (1)-(5) except the shadowing simulation) as a function of the displacement along the measurement path. Results for the active lower Radio Dot are shown in subplot (a), subplot (b) shows results when the upper Radio Dot is active and (c) shows results when both Radio Dots are active. It is worthwhile to note that the fluctuations of

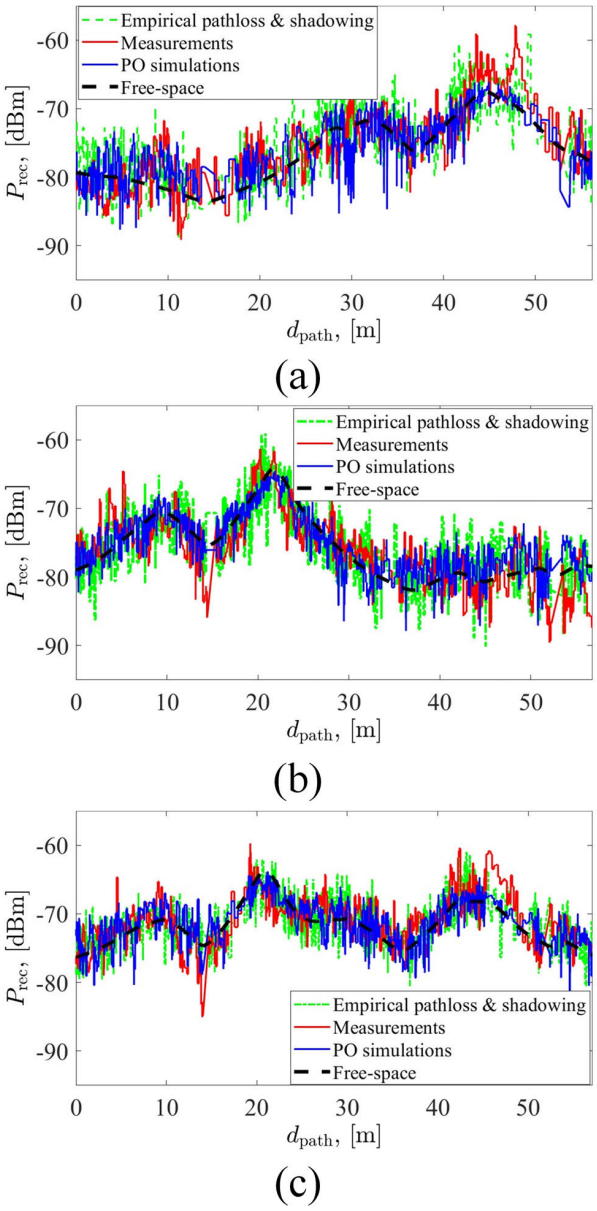

FIGURE 9. Receive power level (RSRP) along the measurement path. The variations as predicted by the different models can be compared with measurements when (a) lover Radio Dot is active, (b) the upper Radio Dot is active and (c) both Radio Dots are active. See Fig. 4 for the Radio Dot positions.

the receive power are lesser for the case when both Radio Dots are active as compared to a single Radio Dot. This is the direct result of diversity gain resulting from combining uncorrelated signals coming from separate transmitters [34]. As expected, the distance trends of the free-space model and the empirical path loss model follow each other very well. However, in practical network deployment, what is important is to be able to predict the fluctuations of the received RSRP levels, which we do next.

Fig. 9 shows the receive power level (RSRP) along the measurement path. The fluctuations as predicted by the different models compared with measurements when (a) the lower Radio Dot is active, (b) the upper Radio Dot is active, and (c) both Radio Dots are active. In all the considered cases we compare data obtained with PO computations with one iteration only. An analysis addressing the number of iterations impact and the complexity of the environment model on the predicted receive power accuracy is outside the scope of this paper and will be published elsewhere in the future.

A quick visual inspection of Fig. 9 suggests that the overall behavior of the predicted signals by means of PO simulations is similar to both measurement data and the empirical path loss plus shadowing model. The reported RSRP is averaged over a certain number of points over time. In order to be able to perform a fair comparison, we have identified the sampling points and the averaging periods and applied them to the simulated data so that they coincide with the measurement data. We have done this for both the PO and the empirical simulations.

Fig. 10 shows the Cumulative Distribution Functions (CDF) of the corresponding data shown in Fig. 9, i.e., the measurement data, the simulated data based on the empirical model, and the simulated data based on the PO computations. Again, visual inspection suggests that the distributions are satisfyingly close to each other. However, we need to quantitatively compare both modeling approaches in terms of their capability to emulate the measurement data. In the analysis below we compare the models with the data with respect to their means μ_{Prec} and standard deviations σ_{Prec}. We also evaluate the root mean squared (RMS) error of the simulated data and the measurement data corresponding to the same receive antenna position along the measurement path RMS_{Prec}. The RMS error inferred from comparing the power corresponding to the same CDF level $\text{RMS}_{\text{Prec@CDF}}$ is also evaluated as indicated in Fig. 10 (a). The correlation coefficient $\boldsymbol{\rho}$ between simulated data and the measurement data has also been computed.

VI. DISCUSSION

A. CAPTURING THE SPATIAL DATA FOR CREATING A DIGITAL ENVIRONMENT

3D scanning has been used for capturing the spatial data of the factory environment in this study and it provides a rapid method for generating a virtual version of the real-world setting of the factory. The method should preferably be performed when there are no other activities in the environment in order to gain the best result and not have any interference or noise in the virtual version. In this case, the scanning could be performed with no disturbances and it required about three hours for the CSI-lab, an area of approximately 261 m^2. To convert the scanning to a point cloud is today an almost automated exercise, which also was the case for this study. The accuracy of the point cloud data is high in comparison to the real-world setting, as was shown in Fig. 3, and distances and dimensions can be extracted directly from the point cloud data. An aspect that was important for this case was the awareness of the materials present in the real-world environment since they impact the scattering of signals,

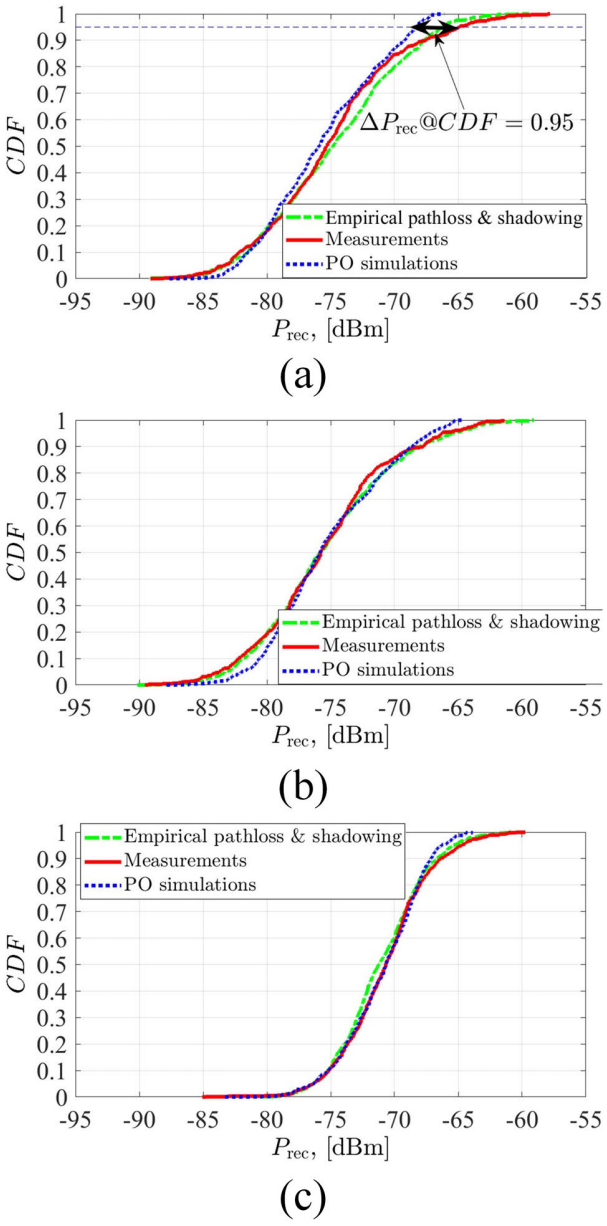

FIGURE 10. Cumulative Distribution Functions (CDF) of the corresponding receive power level (RSRP) as shown in Fig. 10. (a) Lover Radio Dot is active, (b) the upper Radio Dot is active and (c) both Radio Dots are active. See Fig. 4 for the Radio Dot positions.

but there is no information that the point cloud data can provide at this stage and had to be collected manually by documenting.

The desired work procedure would be to use the point cloud data for the simulation since it saves time and the scanning is an automated endeavor, but because it is representing the real-world environment with 3D points, this does not provide the solid surfaces that are required for PO simulations where scattering aspects are considered. As this was a limitation that was encountered during the work and is a known limitation in the research area, a solution was to build a CAD version based on the point cloud data. Building a basic geometry including walls, floor, and infrastructure of the laboratory environment and excluding detailed objects represented in the point cloud was a straightforward procedure in the AutoCAD software. As was stated, the automated generation of objects was disregarded for this case and therefore performed manually by one of the participants in this work. The manual effort implies that when the level of details in the environment increases, so does the time that has to be spent on building the CAD version. The version used for the simulation was one of the simpler models where the simple structures were included, e.g., walls and floor. That the simpler version with low detail level was used, is because it was enough for understanding if the offline approach can produce results that would suggest that it can replace the current procedure of planning a radio network that is of a more ad hoc manner.

Capturing the spatial data involved three steps; 3D scanning in the CSI-lab with 10 scans in total, import the scans for building the point cloud, i.e., the 3D representation generated from the scan, and lastly, building a CAD representation based on the point cloud environment. The two first steps support the generation of a 3D representation in a rapid way with limited interference in the production environment. The real-world representation can be used in an offline mode for understanding what the environment looks like with the placement of equipment and the physical limitations of the location. However, since the simulation requires a model with objects with flat surfaces this limitation had to be overcome by building a CAD representation based on the point cloud data. This has the disadvantage that it requires manual effort and therefore becomes time-consuming as the level of detail increases, compared to being able to use the point cloud data for the simulation. This is a limitation of the technology as of today, but building the CAD version would be required anyhow for the realization of a virtual representation of the environment. In that perspective, the point cloud data, with its high accuracy and photorealistic representation, is a supporting way to be used as a reference when building the CAD model.

B. COMPARISON OF MEASURE AND SIMULATED PERFORMANCE OF THE NETWORK

As can be seen from Table 4, the means μ_{Prec} of the simulated data only negligibly (less than 0.6 dB) differs from the measurement data both for the empirical model and the PO computations. In terms of the standard deviations σ_{Prec}, the results for the empirical simulations differ even less, i.e., 0.1 dB at most, from the measurements. On the other hand, for the PO computations, the maximum observed difference in σ_{Prec} is 1 dB, which is relatively larger, but still sufficiently small in absolute terms. Here we need to keep in mind that the empirical model parameters are obtained from the measurement data, while for the PO computations no measurement data has been used to predict the receive signal levels. Furthermore, if we compare the RMS_{Prec}, we certainly see that the error resulting from the prediction by the PO method is lower or equal to actual measurement data. Also,

TABLE 4. Comparison of PO simulations and empirical simulations with measurement data where L is lower, U is upper, and B is both Radio Dots.

Active RD	M_{PREC} [dBm]	Σ_{PREC} [dBm]	RMS_{PREC} [dB]	ρ	$RMS_{PREC@CDF}$ [dB]
EMPIRICAL					
L	-75.1	5.4	4.3	0.68	0.77
U	-75.7	5.2	4.6	0.62	0.45
B	-71.1	3.4	3.3	0.53	0.44
PO					
L	-75.7	4.4	4.3	0.65	1.49
U	-75.2	4.5	3.8	0.70	0.98
B	-70.9	3.1	3.2	0.53	0.62
MEASURE					
L	-75.1	5.4	0	1	0
U	-75.5	5.2	0	1	0
B	-70.7	3.5	0	1	0

the correlation is rather high between the PO simulations and the measurement data, which is in turn slightly higher than the corresponding value for the empirical modeling approach. On the other hand, if we compare the power corresponding to the same CDF level, we see that the error is larger for the PO computations as compared to the empirical simulations. This can be explained by the slightly lower variance of the power levels predicted by the PO method as compared to the measurement data. The PO computational model results for the prediction of RSRP levels in an indoor factory environment (CSI-lab) were compared to measurements performed in that same environment. The rms error of the received signal power differs only slightly, i.e., up to 1 dB or less for the estimated mean and variance of the predicted receive power as compared to measurements. This value shall be juxtaposed with the reporting accuracy of RSRP measurements which is also 1 dB and the general estimation accuracy of the actual receive signal power provided by RSRP measurements, which is $\pm$ 8 dB.

The proposed PO computational approach offers an error performance that is comparable to predictions obtained from empirical path loss plus shadowing models in terms of both predicted spatial variation as well as statistical distributions. At the same time, the need to perform measurements can be largely reduced, and eventually, as computational methods develop and the computing power increases, almost fully displaced by numerical models.

Despite the excellent agreement between the predicted signal strength and the measurements, a few cautionary words need to be mentioned. Firstly, as well-known, walls and other building structures are not made of PEC materials and are typically modeled as low-loss dielectric materials having dielectric constants in the range of 3-10 depending on frequency [46]. Therefore, further research is needed to find ways to improve signal strength prediction incorporating electric properties of building materials and environment details. Secondly, other modeling approaches can be used instead of the presently adopted PO method, such as GO/UTD methods, that allow for fast computations with complex propagation environment models. A general strategy, regardless of the selected modeling method, i.e., to find an optimal tradeoff between the accuracy and simulation time that will depend on the problem definition and performance metrics of interest. Another practical aspect is the access to suitable simulation software tools and computational platforms for the considered problem and performance metrics – this can vary for different R&D environments. The RSRP measurement results show that the LTE coverage in the investigated scenario, at the CSI-lab, is good, the best signal level is observed in the open hall where the Radio Dots are deployed. This shows that the initial radio to planning prior to deploying the Radio Dots performed by Ericsson is adequate for this kind of deployment scenario.

C. 5G ENABLED MANUFACTURING – INCREASING FLEXIBILITY, EFFICIENCY, AND TRACEABILITY

5G has promising features to support the future factory where equipment and humans will be connected. As has been stressed in this paper, the success of the 5G implementation is dependent on how the values of having the network can exceed the cost involved. The project focuses on how 5G can support increased flexibility, efficiency, and traceability in the manufacturing domain. For the flexibility aspect, this approach enables the network provider to do the planning offline and offsite. An offline network plan can also more easily be updated if changes are requested or if the requirements change. Efficiency is also gained by limiting the interference with ongoing production since the planning can be done in a virtual representation and the downtime for production can be reduced. Another efficiency aspect is the possibility to automate the process and eliminate the need for measuring the network afterward and replacing the more ad hoc way the installation is performed today. As the steps for creating the virtual environment advances and the point cloud data can be used directly in the simulation, it will make the planning process even more efficient and provide high accuracy for performing the planning. For traceability, it will be improved since the planned installation is well documented in the virtual environment and if changes need to be done in a later stage, the digital version is representing reality.

VII. CONCLUSION

The development of an offline approach for radio planning of an indoor environment has been introduced and described in this paper. Furthermore, the simulation results have been verified towards RSRP measurements and show promising results for the applicability of the approach. The RSRP is an essential parameter in the design of LTE wireless networks and the obtained agreement between the numerical computations and measurements is in this study good. Hence, the use of an approach for radio network planning in offline mode is deemed not only feasible but also necessary to cope with the demands and challenges posed by the Fourth Industrial Revolution. Providing an accurate deployment plan will be possible when producing fully automated, cost-efficient, and time-efficient predictions of the network-related physical

parameters like signal strength, interference and noise levels, signal delays, latency, and jitter. As technology advances, a hybrid computational method combining ray-based and PO-based computational methods can be devised. These shall take into account both geometrical and electrical models of large surfaces of the physical environment as well as point cloud data discretization of some objects in a combination of the specification of their electrical characteristics for fine-tuning the prediction of the network-related physical parameters.

The question posed in this paper was ''can a planning approach in offline mode provide the simulation results required for ensuring a reliable and available network in the physical environment?'' The results gained in this paper verify that this is possible. The approach presented here is based on the two existing technology field 3D laser scanning and ray tracing, which separately has high technical maturity, that is combined to address challenges involved in planning a network for an indoor factory environment.

Since this is one of the first attempts to apply this kind of approach for a manufacturing setting, simplifications, and assumptions, such as the geometrical representation and physical entities of the factory environment included, have been made. This in order to serve the purpose to show the applicability of the approach. This means that there are reasons to further investigate this approach and to successively include more aspects that contribute to the complexity. Besides including more complexity in the simulation, would also more use cases in the manufacturing field be needed, both in the case of planning for an existing production system and when designing a new. This approach has real industrial implications and can support ICT providers with more effective network planning processes as the demand for connectivity solutions in manufacturing increases. This has not been studied to a large degree prior to this study but needs further attention by both industry and the research community.

ACKNOWLEDGMENT

The work presented in this paper has been carried out within the Production Area of Advance at Chalmers University of Technology.

REFERENCES

[1] Ericsson. (2016). *More Than 50 Billion Connected Devices*. [Online]. Available: https://www.ericsson.com

[2] A. Osseiran, F. Boccardi, M. Maternia, V. Braun, K. Kusume, P. Marsch, O. Queseth, M. Schellmann, H. Schotten, H. Taoka, H. Tullberg, M. A. Uusitalo, B. Timus, and M. Fallgren, ''Scenarios for 5G mobile and wireless communications: The vision of the METIS project,'' *IEEE Commun. Mag.*, vol. 52, no. 5, pp. 26–35, May 2014, doi: 10.1109/MCOM.2014.6815890.

[3] Ericsson. (2016). Cellular *Networks for Massive IoT-Enabling Low Power Wide Area Applications*. [Online]. Available: https://www.ericsson.com

[4] D. Behnke, M. Müller, P.-B. Bok, and J. Bonnet, ''Intelligent network services enabling industrial IoT systems for flexible smart manufacturing,'' in *Proc. 14th Int. Conf. Wireless Mobile Comput., Netw. Commun. (WiMob)*, Oct. 2018, pp. 1–4.

[5] S. Chen and J. Zhao, ''The requirements, challenges, and technologies for 5G of terrestrial mobile telecommunication,'' *IEEE Commun. Mag.*, vol. 52, no. 5, pp. 36–43, May 2014, doi: 10.1109/MCOM.2014.6815891.

[6] F. E. Idachaba, ''5G networks: Open network architecture and densification strategies for beyond 1000x network capacity increase,'' in *Proc. Future Technol. Conf. (FTC)*, San Francisco, CA, USA, Dec. 2016, pp. 1265–1269.

[7] S. Rangan, T. S. Rappaport, and E. Erkip, ''Millimeter-wave cellular wireless networks: Potentials and challenges,'' *Proc. IEEE*, vol. 102, no. 3, pp. 366–385, Mar. 2014, doi: 10.1109/JPROC.2014.2299397.

[8] Z. Pan, J. Polden, N. Larkin, S. Van Duin, and J. Norrish, ''Recent progress on programming methods for industrial robots,'' *Robot. Comput.-Integr. Manuf.*, vol. 28, no. 2, pp. 87–94, Apr. 2012, doi: 10.1016/j.rcim.2011.08.004.

[9] G. D. L. Roche, A. Alayón-Glazunov, and B. Allen, *LTE-Advanced and Next Generation Wireless Networks: Channel Modelling and Propagation*. Chichester, U.K.: Wiley, 2013.

[10] J. Jarvelainen, K. Haneda, and A. Karttunen, ''Indoor propagation channel simulations at 60 GHz using point cloud data,'' *IEEE Trans. Antennas Propag.*, vol. 64, no. 10, pp. 4457–4467, Oct. 2016, doi: 10.1109/TAP.2016.2598200.

[11] J. Pascual-Garcia, J.-M. Molina-Garcia-Pardo, M.-T. Martinez-Ingles, J.-V. Rodriguez, and L. Juan-Llacer, ''Wireless channel simulation using geometrical models extrated from point clouds,'' in *Proc. IEEE Int. Symp. Antennas Propag. USNC/URSI Nat. Radio Sci. Meeting*, Boston, MA, USA, Jul. 2018, pp. 83–84.

[12] NGMN Alliance, ''5G white paper,'' in *Next Generation Mobile Network's White Paper*, J. Erfanian and B. Daly, Eds. London, U.K.: NGMN Alliance, 2015.

[13] E. Dahlman, S. Parkvall, J. Skold, and P. Beming, *3G Evolution: HSPA and LTE for Mobile Broadband*, 2nd Ed. Oxford, U.K.: Academic, 2008.

[14] *Evolved Universal Terrestrial Radio Access (E-UTRA) and Evolved Universal Terrestrial Radio Access Network (E-UTRAN): Overall Description*, Standard G. T. 36.300, 2011.

[15] B. Bangerter, S. Talwar, R. Arefi, and K. Stewart, ''Networks and devices for the 5G era,'' *IEEE Commun. Mag.*, vol. 52, no. 2, pp. 90–96, Feb. 2014, doi: 10.1109/MCOM.2014.6736748.

[16] W. Chin, Z. Fan, and R. Haines, ''Emerging technologies and research challenges for 5G wireless networks,'' *IEEE Wireless Commun.*, vol. 21, no. 2, pp. 106–112, Apr. 2014, doi: 10.1109/MWC.2014.6812298.

[17] W. Mohr, ''The 5G Infrastructure Public-Private Partnership,'' in *Proc. Presentation ITU GSC Meeting*, 2015, p. 35.

[18] P. Agyapong, M. Iwamura, D. Staehle, W. Kiess, and A. Benjebbour, ''Design considerations for a 5G network architecture,'' *IEEE Commun. Mag.*, vol. 52, no. 11, pp. 65–75, Nov. 2014, doi: 10.1109/MCOM.2014.6957145.

[19] I. Godor, M. Luvisotto, O. Dobrijevic, S. Ruffini, K. Wang, D. Patel, J. Sachs, D. P. Venmani, O. L. Moult, J. Costa-Requena, A. Poutanen, C. Marshall, and J. Farkas, ''A look inside 5G standards to support time synchronization for smart manufacturing,'' *IEEE Commun. Standards Mag.*, vol. 4, no. 3, pp. 14–21, Sep. 2020, doi: 10.1109/MCOMSTD.001.2000010.

[20] M. Peuster, S. Schneider, D. Behnke, M. Muller, P.-B. Bok, and H. Karl, ''Prototyping and demonstrating 5G verticals: The smart manufacturing case,'' in *Proc. IEEE Conf. Netw. Softwarization (NetSoft)*, Jun. 2019, pp. 236–238.

[21] E. A. Oyekanlu, A. C. Smith, W. P. Thomas, G. Mulroy, D. Hitesh, M. Ramsey, D. J. Kuhn, J. D. Mcghinnis, S. C. Buonavita, N. A. Looper, M. Ng, A. Ng'oma, W. Liu, P. G. Mcbride, M. G. Shultz, C. Cerasi, and D. Sun, ''A review of recent advances in automated guided vehicle technologies: Integration challenges and research areas for 5G-based smart manufacturing applications,'' *IEEE Access*, vol. 8, pp. 202312–202353, 2020, doi: 10.1109/ACCESS.2020.3035729.

[22] K. Burow, K. Hribernik, and K.-D. Thoben, ''First steps for a 5G-ready service in cloud manufacturing,'' in *Proc. IEEE Int. Conf. Eng., Technol. Innov. (ICE/ITMC)*, Jun. 2018, pp. 1–5.

[23] Y. Li, D. Wang, T. Sun, X. Duan, and L. Lu, ''Solutions for variant manufacturing factory scenarios based on 5G edge features,'' in *Proc. IEEE Int. Conf. Edge Comput. (EDGE)*, Oct. 2020, pp. 54–58.

[24] H. Yang, Z. Sun, G. Jiang, F. Zhao, X. Lu, and X. Mei, ''Cloud manufacturing-based condition monitoring platform with 5G and standard information model,'' *IEEE Internet Things J.*, early access, Nov. 10, 2020, doi: 10.1109/JIOT.2020.3036870.

[25] E. Dahlman, G. Mildh, S. Parkvall, J. Peisa, J. Sachs, and Y. Selén, "5G Radio Access," *Ericsson Rev.*, vol. 6, pp. 1–8, Jun. 2014.
[26] A. Alexiou, P. Demestichas, and A. Georgakopoulos. (2015). *5G Vision, Enablers and Challenges for the Wireless Future, Outlook Visions and Research Directions for the Wireless World*. WWRF. [Online]. Available: https://www.wwrf.ch/outlook.html
[27] A. Osseiran, V. Braun, T. Hidekazu, P. Marsch, H. Schotten, H. Tullberg, M. A. Uusitalo, and M. Schellman, "The foundation of the mobile and wireless communications system for 2020 and beyond: Challenges, enablers and technology solutions," in *Proc. IEEE 77th Veh. Technol. Conf. (VTC Spring)*, Dresden, Germany, Jun. 2013, pp. 1–5.
[28] M. J. Alarcon, F. J. Zorzano, A. Jevtic, and D. Andina, "Telecommunications network planning and maintenance," in *Proc. 12th World Multi-Conf. Systemics, Cybern. Inform. (WMSCI)*, Orlando, FL, USA, 2008, pp. 1–5.
[29] S. R. Lamas, D. Gonzalez, and J. Hamalainen, "Indoor planning optimization of ultra-dense cellular networks at high carrier frequencies," in *Proc. IEEE Wireless Commun. Netw. Conf. Workshops (WCNCW)*, New Orleans, LA, USA, Mar. 2015, pp. 23–28.
[30] H. Asplund, A. A. Glazunov, A. F. Molisch, K. I. Pedersen, and M. Steinbauer, "The COST 259 directional channel model-part II: Macrocells," *IEEE Trans. Wireless Commun.*, vol. 5, no. 12, pp. 3434–3450, Dec. 2006, doi: 10.1109/TWC.2006.256967.
[31] U. T. Virk, S. L. H. Nguyen, K. Haneda, and J.-F. Wagen, "On-site permittivity estimation at 60 GHz through reflecting surface identification in the point cloud," *IEEE Trans. Antennas Propag.*, vol. 66, no. 7, pp. 3599–3609, Jul. 2018, doi: 10.1109/TAP.2018.2829798.
[32] K. A. Remley, H. R. Anderson, and A. Weisshar, "Improving the accuracy of ray-tracing techniques for indoor propagation modeling," *IEEE Trans. Veh. Technol.*, vol. 49, no. 6, pp. 2350–2358, Nov. 2000, doi: 10.1109/25.901903.
[33] A. M. Hammoudeh and G. Allen, "Millimetric wavelengths radiowave propagation for line-of-sight indoor microcellular mobile communications," *IEEE Trans. Veh. Technol.*, vol. 44, no. 3, pp. 449–460, Aug. 1995, doi: 10.1109/25.406611.
[34] P.-S. Kildal, *Foundations of Antennas: A Unified Approach for Line-of-Sight and Multipath* (Compendium Antenna Eng). Gothenburg, Sweden: Kildal Antenn AB, 2013.
[35] A. A. Glazunov, Z. Lai, and J. Zhang, "Outdoor-indoor channel," in *LTE-Advanced and Next Generation Wireless Networks: Channel Modelling and Propagation*, G. D. L. Roche, A. Alayón-Glazunov, and B. Allen, Eds. Chichester, U.K.: Wiley, 2013, pp. 123–151.
[36] O. A. Iupikov, R. Maaskant, M. V. Ivashina, A. Young, and P.-S. Kildal, "Fast and accurate analysis of reflector antennas with phased array feeds including multiple reflections between feed and reflector," *IEEE Trans. Antennas Propag.*, vol. 62, no. 7, pp. 3450–3462, Jul. 2014, doi: 10.1109/TAP.2014.2320529.
[37] O. A. Iupikov, C. Craeye, R. Maaskant, and M. V. Ivashina, "Domain-decomposition approach to Krylov subspace iteration," *IEEE Antennas Wireless Propag. Lett.*, vol. 15, pp. 1414–1417, Dec. 2016, doi: 10.1109/LAWP.2015.2511195.
[38] T. Várady, R. R. Martin, and J. Cox, "Reverse engineering of geometric models—An introduction," *Comput.-Aided Des.*, vol. 29, no. 4, pp. 255–268, Apr. 1997.
[39] J. Berglund, E. Lindskog, and B. Johansson, "On the trade-off between data density and data capture duration in 3D laser scanning for production system engineering," *Procedia CIRP*, vol. 41, pp. 697–701, Feb. 2016, doi: 10.1016/j.procir.2015.12.141.
[40] Z. M. Bi and L. Wang, "Advances in 3D data acquisition and processing for industrial applications," *Robot. Comput.-Integr. Manuf.*, vol. 26, no. 5, pp. 403–413, Oct. 2010, doi: 10.1016/j.rcim.2010.03.003.
[41] L. Klein, N. Li, and B. Becerik-Gerber, "Imaged-based verification of as-built documentation of operational buildings," *Autom. Construct.*, vol. 21, pp. 161–171, Jan. 2012, doi: 10.1016/j.autcon.2011.05.023.
[42] FARO Technologies. (2011). *FARO Laser Scanner Focus 3D Manual*. [Online]. Available: https://doarch332.files.wordpress.com/2013/11/e866_faro_laser_scanner_focus3d_manual_en.pdf
[43] O. Iupikov, "Digital beamforming focal plane arrays for radio astronomy and space-borne passive remote sensing," Ph.D. dissertation, Dept. Elect. Eng., Chalmers Univ. Technol., Gothenburg, Sweden, 2017.
[44] S. Grubisic and W. P. Carpes, "An efficient indoor ray-tracing propagation model with a quasi-3D approach," *J. Microw., Optoelectron. Electromagn. Appl.*, vol. 13, no. 2, pp. 166–176, Dec. 2014.
[45] F. S. D. Adana, O. G. Blanco, I. G. Diego, J. P. Arriaga, and M. F. Catedra, "Propagation model based on ray tracing for the design of personal communication systems in indoor environments," *IEEE Trans. Veh. Technol.*, vol. 49, no. 6, pp. 2105–2112, Nov. 2000.
[46] Recommendation ITU-R P.2040. *Effects of Building Materials and Structures on Radiowave Propagation Above About 100 MHz*. Accessed: Dec. 21, 2020. [Online]. Available: https://www.itu.int/rec/R-REC-P.2040-1-201507-I/en

MAJA BÄRRING was born in Gothenburg, Sweden, in September 1988. She received the M.Sc. degree in mechanical engineering from the Faculty of Engineering, Lund University, in 2014. She is currently pursuing the Ph.D. degree with the Production Systems Division, Industrial and Materials Science, Chalmers University of Technology.

During her engineering studies, she has participated in an ERASMUS Exchange Program at the Technical University of Berlin (TUBerlin) from 2011 to 2012. After graduation, she was enrolled as a Graduate Trainee at Siemens in both Sweden and the US for two years, gaining industrial experiences from manufacturing. Her research topic is on how more data representing the production system enabled by digital technologies provide values to the production organization. The research focuses on how the data in itself and as decision support provide values. The research projects are focused on the use of digital technologies in the production environment, such as 5G connectivity in the workshop, 3D scanning for capturing the spatial data, Digital Twin technology for creating digital copies of production systems, platforms for enabling new business opportunities, and market places, and blockchain to ensure secure data sharing in the supply chain case. She has spent six months of her Ph.D., autumn 2019, at the Systems Integration Division, National Institute of Standards and Technology (NIST), USA, as a Guest Researcher. The focus during this exchange was a technical development of how to enable the exchange of machine model data on a neutral standard format to support information reuse and interoperability between systems. Parallel with the research exchange, she has also been enrolled in national and international standardization bodies (ISO) as an expert from Sweden in topics related to manufacturing data. The current standard that has priority is within ISO is ISO 23247 "Digital Twin Framework for Manufacturing."

OLEG IUPIKOV (Member, IEEE) received the M.Sc. degree *(cum laude)* in electrical engineering from the Sevastopol National Technical University, Ukraine, in 2006, and the Ph.D. degree from the Chalmers University of Technology, Gothenburg, Sweden, in 2017.

After graduating, he was working at the Radio Engineering Bureau, Sevastopol. During this period, he was also a Visiting Researcher at The Netherlands Institute for Radio Astronomy (ASTRON), where he was involved in the development of the focal plane array simulation software for the APERTIF radio telescope. This visit was funded by the SKADS Marie Curie Visitor Grant and the APERTIF project. He currently works as a Postdoctoral Researcher with the Chalmers University of Technology. His research interests are receiving antenna array systems, in particular focal plane arrays for radio astronomy and microwave remote sensing applications, numerical methods for their analysis and optimization, signal processing algorithms for antenna systems, and integration of antennas with active components. He has authored/coauthored over 40 journal and conference papers.

ANDRÉS ALAYÓN GLAZUNOV (Senior Member, IEEE) was born in Havana, Cuba. He received the M.Sc. (Engineer-Researcher) degree in physical engineering from Peter the Great St. Petersburg Polytechnic University (Polytech), St. Petersburg, Russia, in 1994, the Ph.D. degree in electrical engineering from Lund University, Lund, Sweden, in 2009, and the Docent (Habilitation) qualification in antenna systems from the Chalmers University of Technology, Gothenburg, Sweden, in 2017.

From 1996 to 2005, he held various research and specialist positions in the Telecom industry, e.g., Ericsson Research, Telia Research, and TeliaSonera, Stockholm, Sweden. From 2001 to 2005, he was the Swedish delegate to the European Cost Action 273. From 2018 to 2020, he was the Dutch Delegate to the European Cost Action IRACON. He has been one of the pioneers in producing the first standardized OTA measurement techniques for 3GPP, and devising novel OTA techniques, i.e., the Random-LOS and the Hybrid antenna characterization setups. He has contributed to, or initiated various European research projects, i.e., more recently, the is3DMIMO, the WAVECOMBE and the Build-Wise projects under the auspices of the H2020 European Research and Innovation program. He has also contributed to the international 3GPP and the ITU standardization bodies. From 2009 to 2010, he held a Marie Curie Senior Research Fellowship at the Centre for Wireless Network Design, University of Bedfordshire, Luton, U.K. From 2010 to 2014, he held a postdoctoral position with the Electromagnetic Engineering Laboratory, KTH-Royal Institute of Technology, Stockholm. From 2014 to 2018, he held an Assistant Professor position at the Chalmers University of Technology. He is currently an Associate Professor with the Department of Electrical Engineering, University of Twente, Enschede, The Netherlands, where he is leading the Radio, Propagation and Antenna Systems research. And he is also an Affiliate Professor with the Chalmers University of Technology, where he is leading the OTA Characterization of Antenna Systems research area. He is the author of more than hundred scientific and technical publications. He is the coauthor and coeditor of the text book *LTE-Advanced and Next Generation Wireless Networks – Channel Modelling and Propagation* (Wiley, 2012). His current research interests include, but are not limited to mmWave array antenna design, MIMO antenna systems, electromagnetic theory, fundamental limitations on antenna-channel interactions, radio propagation channel measurements, modeling and simulations, wireless performance in the built environment, and the OTA characterization of antenna systems and wireless devices.

MARIANNA IVASHINA (Senior Member, IEEE) received the Ph.D. degree in electrical engineering from the Sevastopol National Technical University (SNTU), Ukraine, in 2001.

From 2001 to 2010, she was with The Netherlands Institute for Radio Astronomy (ASTRON), where she carried out research on innovative phased array technologies for future radio telescopes, such as the Square Kilometer Array. From 2002 to 2003, she has also stayed as a Visiting Scientist with the European Space Agency, ESTEC, where she studied multiple-beam array feeds for the satellite telecommunication system Large Deployable Antenna. In January 2011, she joined the Chalmers University of Technology, Gothenburg, Sweden, where she is currently a Full Professor and the Head of the Antenna Systems Group, Department of Electrical Engineering. Her current research interests include antenna array systems, integration of antennas with active electronic components, synthesis of aperiodic arrays, and other unconventional array architectures, reflector antennas, and focal plane array feeds. She has published extensively on the above topics, having authored/coauthored over 130 journal and conference papers.

Prof. Ivashina has received several scientific awards, including the URSI Young Scientists Award for GA URSI, Toronto, Canada (1999), the APS/IEEE Travel Grant, Davos, Switzerland (2000), the 'Best Team Contribution' Paper Award at the ESA Antenna Workshop (2008), the EU FP7 Marie Curie Actions International Qualification Fellowship (2009), the Best Paper Award at the IEEE COMCAS Conf., Tel-Aviv, Israel (1019)], and numerous research project funding grants from Swedish and European funding agencies. She is currently an Associate Editor of the IEEE Transactions on Antennas and Propagation and a Board Member of the European School of Antennas (ESoA). Since 2021, she has been the Delegate of the European Association of Antennas and Propagation (EurAAP) for Region 6: Iceland, Norway, and Sweden.

JONATAN BERGLUND was born in Gothenburg, Sweden, in January 1983. He received the M.Sc. degree in production engineering from the Chalmers University, Gothenburg, Sweden, in 2010.

As a Ph.D. student at the Chalmers University of Technology since 2013, he has done research on the application of 3D-scanning technology in manufacturing engineering projects across several different industries. Following his engineering studies, he spent a year as a Guest Researcher (2010–2011) in the Manufacturing Systems Integration Division, National Institute of Science and Technology, Gaithersburg, MA, USA, where he worked on Discrete Event Simulation modeling approaches for predicting and reducing environmental effects of manufacturing operations. In December 2018, he co-founded Visinator AB, a technology consultancy company working with developing the digitalization capabilities of Swedish manufacturing SME's, where he is managing the metrology and 3D-imaging operations of the company.

BJÖRN JOHANSSON was born in Gothenburg, Sweden, in November 1975. He received the Ph.D. degree in production engineering from the Department of Materials and Manufacturing Technology, Chalmers University of Technology, Gothenburg, Sweden, in 2006.

He performs research on the area of how digitalization can aid manufacturing industries to achieve a more sustainable society at large. His areas of interest are circular economy and sustainable development, and in this context how digital tool such 5G, 3D scanning, discrete event simulation, artificial intelligence, virtual and augmented reality can be applied for manufacturing industries. He joined the Department of Product and Production Development, Chalmers University of Technology, in 2006, as an Assistant Professor, as an Associate Professor (2011), and as a Professor in Sustainable Production (2015). He is currently the Director of PMC Europe AB and the Director of the Board at The Society of Modeling and Simulation International. He worked as a Guest Researcher at the National Institute of Standards and Technology (2007–2010) and (2015–2016). He is currently working as the Vice Head of the Division of Production Systems, Department of Industrial and Materials Science, Chalmers University of Technology, Gothenburg.

Dr. Johansson is an active member of the AAAS, ACM, and SCS. He received the Swedish Royal Academy of Science Award in Technology 2004, C-SELT 2004, Alde Nilsson ABB Award in 2003, the Ernst Gerber Jubilee Fund in 2003, and the Chalmers Foundation Scholarship in 2002. He was the General Chair for the Winter Simulation Conference sponsored by the IEEE during 2018 in Gothenburg, as well as the Co-Editor (2009) and the Lead Editor (2010).

JOHAN STAHRE received the M.Sc. degree in production engineering from the Linköping University of Technology, in 1987, and the Ph.D. degree from the Chalmers University of Technology, in 1995, within the field of manufacturing automation.

Since 2005, he has been the Professor (Chair) and the Head of the Division of Production System at Chalmers. He is also the Vice Head of the Department of Industrial and Materials Science, responsible for research utilization and innovation. He has a long track record of international publication as well as national and international research projects. He was a main driver behind the national Strategic Research Area for Manufacturing in Sweden 2009, later serving as its Co-Director at the Chalmers node, Sustainable Production Initiative, for eight years. He was also the main author of the winning proposal for the 12-year national Swedish Research and Innovation Programme – Produktion2030, and he has been its Co-Director, since 2013. In 2018, he was in the core group of partners developing the winning proposal for the EIT Manufacturing Grant of 450 M. Later, he became its interim Director of Innovation and interim CEO of EIT Manufacturing Colocation Centre North. He has frequently served as the Expert Advisor to industry and to the Swedish Government and has been an advisor to the European Commission and the World Economic Forum in questions related to manufacturing and the future of digitalization and jobs.

FREDRIK HARRYSSON (Senior Member, IEEE) received the M.S. degree in electrical engineering from the Chalmers University of Technology, Gothenburg, Sweden, in 1994, and the Licentiate and Ph.D. degrees in radio systems engineering from Lund University, Lund, Sweden, in 2009 and 2012, respectively.

From 1994 to 1995, he was a Research Engineer with the Department of Microwave Systems, Swedish Defense Research Establishment, Linköping, where he was involved with wideband microwave circuits. In 1995, he joined the Antenna Department at Ericsson Microwave Systems AB in Gothenburg, working mainly with the modeling of large array antennas for airborne radar systems. The department later from 1998 became a part of Ericsson Research, Ericsson AB, where, since then, he has been mainly involved with modeling and measurements of antennas and radio wave propagation for mobile communications. Since 2006, he has been engaged with an industrial Ph.D. project at Lund University, resulting in his Ph.D., in 2012, working on channel modeling with a focus on user effects on terminal antennas, vehicle communication, and outdoor-to-indoor propagation. His research interests mainly concerned the interaction between antennas, propagation, and scattering in the mobile radio channels. Since 2017, he has been working as a Research Unit Manager at the Department for Electronics and EMC, RISE Research Institutes of Sweden, Borås. His current research interests still involve antennas, propagation, and channel modeling for wireless communication, but also EMC and test and validation methods.

ULRIKA ENGSTRÖM received the M.Sc. and Ph.D. degrees in physics and engineering physics from the Chalmers University of Technology, Gothenburg, Sweden, in 1994 and 1999, respectively. Since then, she has been with Ericsson Research driving key research projects and testbed development targeting 4G and 5G research. She holds more than ten patents. Her current research interests include deployments of cellular systems (4G, 5G), radio spectrum, and also new use cases.

MARTIN FRIIS received the M.Sc. degree in mechanical engineering from Lund University, Sweden, in 1996, the Ph.D. degree in materials science from Lund University, in 2003, and the executive MBA degree from the University of Gothenburg School of Business, Economics and Law, Sweden, in 2018.

He held a postdoctoral position at the Center for Thermal Spray, Stony Brook University, New York, NY, USA, from 2003 to 2005. From 2005 to 2018, he worked at SKF with R&D and innovation in managerial positions. He currently runs his own consultancy company, Nuqi Knowledge AB, Gothenburg, Sweden. He holds two patents and is a member of the strategic innovation platform Production 2030 in Sweden.